VARICOSE, a WD-domain protein, is required for leaf blade development

Michael K. Deyholos[2], G. Frank Cavaness[1], Branden Hall[1], Ed King[1], Jayson Punwani[1], Jaimie Van Norman[1] and Leslie E. Sieburth[1,*]

[1]Department of Biology, University of Utah, Salt Lake City, Utah, 84112, USA
[2]Department of Biological Sciences, University of Alberta, Edmonton, AB, Canada T6G 2E9
*Author for correspondence (e-mail: sieburth@biology.utah.edu)

Accepted 10 September 2003

Development 130, 6577-6588
Published by The Company of Biologists 2003
doi:10.1242/dev.00909

Summary

To gain insight into the processes controlling leaf development, we characterized an *Arabidopsis* mutant, *varicose* (*vcs*), with leaf and shoot apical meristem defects. The *vcs* phenotype is temperature dependent; low temperature growth largely suppressed defects, whereas high growth temperatures resulted in severe leaf and meristem defects. *VCS* encodes a putative WD-domain containing protein, suggesting a function involving protein-protein interactions. Temperature shift experiments indicated that VCS is required throughout leaf development, but normal secondary vein patterning required low temperature early in leaf development. The low-temperature *vcs* phenotype is enhanced in *axr1-3 vcs* double mutants and in *vcs* mutants grown in the presence of polar auxin transport inhibitors, however, *vcs* has apparently normal auxin responses. Taken together, these observations suggest a role for VCS in leaf blade formation.

Key words: Leaf Development, Vein Pattern, WD domain, Meristem, *Arabidopsis thaliana*

Introduction

Leaves are composed of a leaf blade, a broad flat structure that is specialized for photosynthesis, and a petiole, a stem-like structure that attaches the blade to the stem. A prominent feature of the leaf blade is its thick central midrib, which extends from the petiole and contains vascular tissues as well as enlarged supporting cells on the abaxial surface of the leaf. Surrounding the midrib is the lamina, which consists of patterned arrays of specialized cell types. Efforts in many labs to identify the molecules that are essential for normal leaf development are beginning to elucidate the pathways that are required for formation of a normal leaf, however, much information is still lacking.

Leaf primordia arise as radial pegs on the flank of the shoot apical meristem (SAM), and become flattened early in development, indicating acquisition of abaxial/adaxial polarity. These steps are rapidly followed by the outgrowth of the leaf blade and differentiation of specialized cell types (Pyke et al., 1991; Carland and McHale, 1996; Donnelly et al., 1999; Medford et al., 1992). *Arabidopsis* genes whose products are proposed to play a role in polarity establishment have been identified based on mutant phenotypes (McConnell and Barton, 1998; Kerstetter et al., 2001; Siegfried et al., 1999; Eshed et al., 2001; McConnell et al., 2001). These studies implicate separate sets of genes for specification of adaxial and abaxial leaf domains.

The importance of abaxial/adaxial polarity for leaf architecture has been revealed by both mutant phenotypes and ectopic expression of polarity genes. Dominant *phb* mutants produce radialized leaves composed entirely of adaxial tissue (McConnell and Barton, 1998) and ectopic *KANADI* expression results in radialized leaves composed entirely of abaxial tissues (Kerstetter et al., 2001; Eshed et al., 2001). The defects in these radialized leaves include leaf morphology and specification of epidermal and internal tissues. These and other studies have contributed to a model for leaf blade outgrowth as a down-stream event following juxtaposition of adaxial and abaxial cell types.

While lamina outgrowth appears to be initiated by acquisition of polarity, the final shape of a leaf appears to be governed by a host of additional factors. For example, leaf cell polar elongation contributes to leaf shape, as cell elongation mutants produce leaves that are either narrower or shorter than the wild type (Tsuge et al., 1996). This polar expansion and shape change appear to be related to altered control of the cytoskeleton, as the leaf cell expansion mutant *an1* has defects in organization of cortical microtubules (Kim et al., 2002). Over-expression of *KNOX* genes also leads to leaf shape defects, presumably through altered regulation of GA biosynthesis (Ori et al., 2000; Chuck et al., 1996; Byrne et al., 2000; Sakamoto et al., 2001; Hay et al., 2003).

The plant hormone auxin has also been implicated in leaf development. Auxin is synthesized is apical portions of the plant, and actively transported basipetally (reviewed by Muday and DeLong, 2001). *Arabidopsis* mutants with defects in auxin transport or auxin responses also produce leaves with altered morphology. For example, the *lop1* mutant produces small asymmetric leaves with disrupted vascular development and it has reduced polar auxin transport (Carland and McHale, 1996). Similarly, the *pin1* mutant, which has a lesion in a putative auxin efflux carrier, and the *tir3* mutant, which has reduced auxin transport, both produce leaves with morphological

defects (Okada et al., 1991; Ruegger et al., 1997). Leaf development is also perturbed by growing wild-type plants in the presence of polar auxin transport inhibitors (Mattsson et al., 1999; Sieburth, 1999). Furthermore, some auxin-resistant mutants, such as *axr1* and *axr2-1*, have disrupted auxin responses and also produce misshapen leaves (Estelle and Somerville, 1987; Timpte et al., 1994). The combined altered leaf shape and perturbed auxin processes in all these examples provides strong evidence that auxin plays a role in leaf development. However, with the exception of *lop1*, detailed anatomical characterization of the leaf developmental defects are lacking.

Although the role of auxin in leaf morphogenesis is not understood, a large body of work implicates polar transport of auxin as an inductive signal for vein formation (reviewed by Sachs, 1981; Aloni, 1987). In leaves, both auxin antibodies and the auxin responsive reporter gene DR5 show auxin to be largely localized in procambial cells (precursors to vascular cell types) as leaf veins are formed (Avsian-Ketchmer et al., 2002; Aloni et al., 2003; Mattsson et al., 2003). However, whether the varied leaf morphologies described for auxin-related mutants is due to effects on vascular tissue or effects on other aspects of leaf development is not known.

Here we describe *varicose* (*vcs*) mutants, which show pleiotropic temperature dependent developmental defects in leaves and the meristem. *VCS* encodes a putative WD domain protein, and each of the five *vcs* alleles we identified has a lesion expected to produce a null allele. The *vcs* leaf phenotype is enhanced under conditions in which auxin signaling is perturbed, but no defects in auxin signaling itself is detectable in *vcs* mutants. These observations led us to propose that VCS and a pathway perturbed by polar auxin transport inhibitors play partially redundant roles in leaf blade formation.

Materials and methods

Plant growth and genetic analyses

Seedling growth and mutagenesis were carried out as described previously (Deyholos et al., 2000). Plant age indicates the time from placement into growth chambers. Lateral root numbers were determined microscopically; counts included all incipient roots that penetrated the epidermis. Phenotypic analyses were based on observations of at least 50 samples, and representative examples are used in the figures.

We used web based resources to find a mutation in the *VCR* gene (Salk_002338) (Alonso et al., 2003). For analyzing the *axr1-3 vcs-1* double mutant, control crosses (*vcs* × Col-0) were carried out and analyzed in parallel. *axr1-3 vcs-1* double mutants were obtained from the self-pollinated (F3) progeny of auxin-resistant F_2 plants.

Polar auxin transport inhibition experiments used growth medium supplemented with N-1-naphthylphthalamic acid (NPA, Chemserv) dissolved in dimethyl sulfoxide (Sigma), and DMSO-supplemented growth medium (GM) used as a control.

Root elongation assays

Wild type and *vcs* seeds were germinated on vertical hormone-free GM for 5 (16°C) or 3 (29°C) days, then 11-20 seedlings of each genotype per treatment were transferred to fresh GM supplemented with indole-3-acetic acid (IAA; Sigma) (10^{-6} M to 10^{-12} M in 0.1× serial dilutions). We measured the root length after 3 days growth at the same temperature. The dose of IAA that caused 50% inhibition of root elongation (I_{50}) was determined using linear regression (Maher and Martindale, 1980).

Molecular characterization

Mapping of *VCS* used 750 F_2 plants from a cross of *vcs-1* heterozygotes to a plant of the Columbia ecotype. We isolated DNA from homozygous mutant F_2 plants (Dellaporta et al., 1983). Polymorphic PCR-based markers were used to map recombination breakpoints (Bell and Ecker, 1994; Konieczny and Ausubel, 1993). Markers included polymorphisms identified by CEREON (Jander et al., 2002), details about primer sequences and polymorphisms are available upon request. Candidate genes within the identified interval were amplified from DNA isolated from each mutant allele, and the PCR products were sequenced using the University of Utah sequencing facility. DNA sequences were assembled and analyzed using JELLYFISH (LabVelocity, San Francisco). The homolog from humans has the accession no. NP_055144, and that from *Drosophila*, accession no. NP_609486.

The pVCS::GUS gene fusion was constructed using a 980 bp fragment (extending between the 3′UTR of the upstream gene and the *VCS* transcription start site), amplified using primers that introduced *Hin*dIII and *Bam*HI restriction sites (5′: CTGCAGGGATCCATC-TCGCTCTCTCTGTTTCTTC and 5′: CACTGTAAGCTTAGATT-TTTTGCAGATTTAAGATCG). This fragment was cloned into pCambia1381z, and sequenced to identify clones containing no mutations. The resulting plasmid was introduced into *Agrobacterium tumifaciens* LBA4404. Wild-type Columbia and Landsberg *erecta* plants were transformed by floral dip (Clough and Bent, 1998). GUS staining, driven by the *VCS* upstream region (pVCS::GUS) was analyzed in 12 independent transformants, and compared to seven independent transformants carrying the empty vector. Ten of the twelve pVCS::GUS lines produced an identical expression pattern; six empty vector controls gave no expression, and one gave faint staining in hydathodes and the root apex.

RT-PCR

RT-PCR was carried out using the Promega Reverse Transcription System kit, and oligo(dT) for first strand synthesis. Amplification used primers within exon 6 (3980F: 5′: GGTCCCGGTTTGTCATCTAC) and within exon 11 (5931R: 5′:CTGTAGGGCCGAAGTGAAAG). Control reactions used primers for α tubulin as described by Semiarti et al. (Semiarti et al., 2001). RNA was isolated from roots, hypocotyls, cotyledons and apex (leaves plus meristem) of 8-day seedlings, 12-day whole seedlings and assorted siliques from mature L*er* plants (all grown at 22°C) using the RNeasy kit from Qiagen.

Microscopy

Tissue for dark-field and DIC microscopy were fixed in a solution of ethanol and acetic acid (3:1), and cleared in saturated chloral hydrate. Tissue preparation for CLSM followed the method of Running (Running, 2002). Tissue for SEM was prepared as described by Chen et al. (Chen et al., 1999). Leaf vein development was assessed in chloral-hydrate-cleared first leaf pairs by visual inspection using 200 and 400× DIC microscopy. We examined both leaves of 12-16 seedlings, per time point. Procambium was recognized as files of elongated cells in positions expected for veins, and a vein counted as differentiated if tracheary elements were present.

GUS staining

Tissue was fixed for 10 minutes in cold 90% acetone, and stained for 3-10 hours at 37°C in 2 mM 5-bromo-4-chloro-3-indoxyl-β-D-glucuronide, 50 mM sodium phosphate, pH 7.0; 5 mM $K_3/K_4Fe(CN)_6$, 0.1% (w/v) Triton X-100. Following staining, samples were rinsed in water for 1-3 hours, fixed overnight in a 6:1 solution of ethanol:acetic acid, and cleared in saturated chloral hydrate.

Results

To investigate leaf development, we isolated five alleles of a

recessive mutant that produced defective leaves. This mutant, *varicose* (*vcs*), was smaller than the wild type, and produced narrow, asymmetric leaves when grown at 22°C (Fig. 1A-C). All five mutant alleles showed identical phenotypic responses to growth temperature. When grown at 16°C, *vcs* mutants resembled the wild-type controls except their leaves were pointed at the apex, and prolonged growth revealed defects in apical dominance (Fig. 1D-F). In contrast, growth at 29°C resulted in a strongly enhanced phenotype. These high-temperature-grown mutants were chlorotic, leaves were narrow and epinastic, and prolonged growth resulted in a callus-like growth at the apex (Fig. 1G-I). *vcs* roots appeared similar to those of wild type, except that at high temperature root hairs occasionally appeared swollen (Fig. 1J-P). *vcs* also produced decreased numbers of lateral roots (Table 1). The decrease in lateral root formation in *vcs* mutants might be a secondary consequence of *vcs* apical defects, as normal lateral root formation requires shoot-derived auxin (Reed et al., 1998).

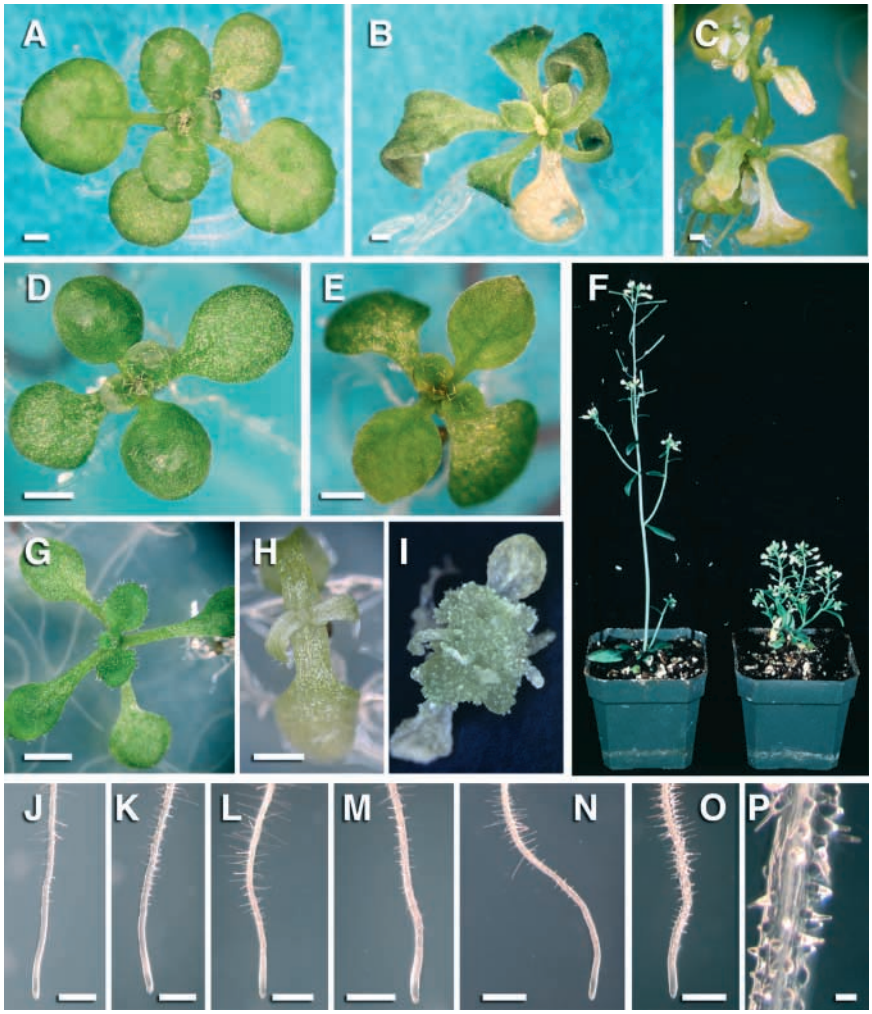

Fig. 1. *vcs* mutants show temperature-dependent defects in leaf development. (A-C) Plants grown at 22°C; 15-day wild type (A) has broad leaves, whereas the 15-day *vcs* mutant (B) produces narrow curled leaves. Following prolonged growth (C; 25-day shown), *vcs* develops flowers, but no seeds are produced. (D-F) Plants grown at 16°C; 16-day wild type (D) produces broad leaves, and the 16-day *vcs* produces broad, but pointed leaves (E). At this temperature, *vcs* can be grown on soil, produce flowers and set seed (F), but the mutant plant has short inflorescence stems and reduced apical dominance (wild type on the left and *vcs* on the right). (G-I) Plants grown at 29°C; 11-day wild type produces broad leaves (G), whereas the 11-day *vcs* mutant appears chlorotic and produces small epinastic leaves (H). Prolonged growth at 29°C in *vcs* results in a few additional leaf-like organs, and an enlarged callus-like apex (I). (J-P) Roots of wild type and *vcs* mutants: (J,K) 16°C-grown 7-day wild type and *vcs*, respectively; (L,M) 22°C-grown 4-day wild type and *vcs*, respectively; (N-P) 29°C-grown 4-day wild type (N) and *vcs* (O,P). A high magnification image of the *vcs* root (P) shows the swollen root hairs. Scale bars: (A-O) 1 mm; (P) 100 μm.

VCS is required for normal meristem and leaf development

The aberrant leaves formed in *vcs* mutants could result from a requirement for VCS function in leaf development alone, in meristem function, or in both. To distinguish between these possibilities, we first characterized the *vcs* SAM. The wild-type SAM was similar in size and organ phyllotaxy regardless of growth temperature (Fig. 2A-C). In contrast, the *vcs* SAM was smaller than the wild type; this defect was most severe in the 29°C-grown *vcs* plants, where the SAM appeared small and flat (Fig. 2D-F). The smaller *vcs* meristem was surprising, given the enlarged appearance of *vcs* apex following prolonged growth at 29°C (Fig. 1I). To reconcile these observations, we compared sections of 14-day 29°C-grown wild type and *vcs* apices. These *vcs* apices contained multiple clusters of small densely staining cells dispersed across the apical region and often in close proximity to leaf-like structures, but no typical SAM (Fig. 2G-H). We also examined younger *vcs* SAMs using CLSM (Fig. 2I-J). *vcs* SAMs were smaller than the wild-type ones, the cells were somewhat vacuolated, and they lacked the layered organization typical of the wild type. Taken together, these data suggested that *VCS* is required for SAM maintenance.

A role for VCS in leaf development can be inferred because *vcs* mutants produce narrow and misshapen leaves; to fully characterize these leaf defects, we examined both internal and epidermal tissues. Leaves typically contain a single layer of

Table 1. Average lateral root numbers for 7-day *vcs* and L*er* plants

	vcs	L*er*
16°C	0.8 (15)	4.3 (17)
22°C	0.6 (25)	8.2 (25)
29°C	0 (22)	10.4 (12)

Number counted is indicated in parentheses.

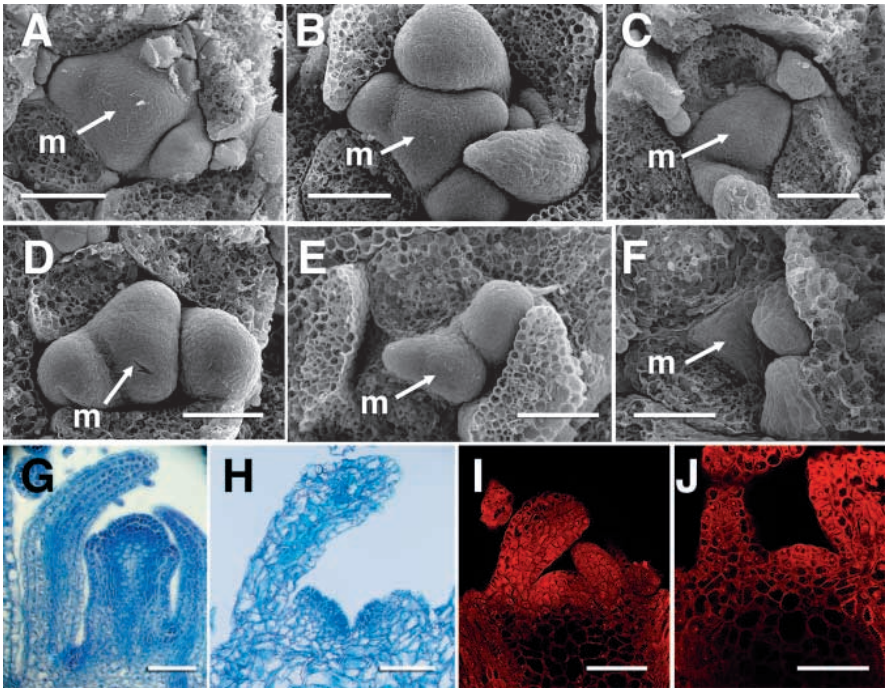

Fig. 2. *vcs* mutants have reduced SAM size. (A-F) SEM images of the SAM (all shown at the same magnification) of L*er* (A-C) and *vcs* (D-F) from seedlings grown at 16°C for 15 days (A,D), 22°C for 12 days (B,E) and 29°C for 9 days (C,F). (G,H) Toluidine Blue-stained paraffin section of 14-day 29°C-grown L*er* (G) and *vcs-1* (H). (I,J) CSLM images of meristems from 7-day 29°C-grown L*er* (I) and *vcs* (J). m indicates meristem. Scale bars: (A-F, I,J) 50 μm; (G,H) 100 μm.

elongated palisade parenchyma cells underlying the adaxial epidermis, beneath which is spongy parenchyma, composed of cells and air spaces. These tissues were apparent in sections of wild-type leaves (Fig. 3A-C). In contrast, 29°C-grown *vcs* leaves contained irregularly spaced cells of variable size (Fig. 3D). The 22°C-grown *vcs* leaves also contained no distinct palisade parenchyma layer, and the 16°C-grown *vcs* leaf palisade parenchyma cells were less densely packed than in the wild-type controls (Fig. 3E,F). We also examined leaf vein pattern. Normal *Arabidopsis* leaves contain a single primary vein that extends the length of the leaf, between five and eight secondary veins that intersect subjacent to the margin to define a series of closed loops called areoles, and minor veins that further subdivide the leaf area (Fig. 3G,I,K). When grown at 22°C, *vcs* leaves contained fewer veins than the wild type, and these veins were both thicker than the wild type and aberrantly patterned (Fig. 3G-H,M-N). When grown at 29°C, *vcs* leaves contained a single primary vein, and up to three small secondary veins, whereas 16°C grown *vcs* leaves had a nearly wild-type vein pattern (Fig. 3I-L).

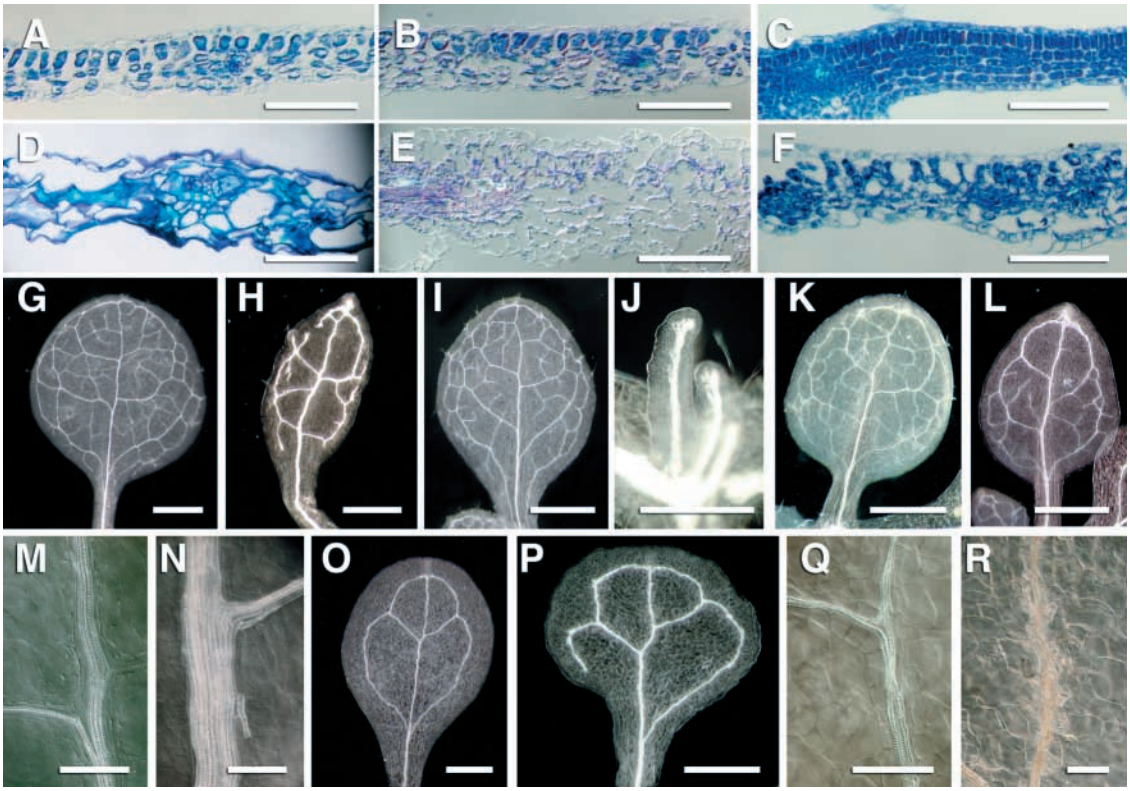

Fig. 3. Leaf defects in internal tissues of *vcs* mutants. (A-F) Cross sections of the first leaf from 12-day L*er* (A-C) and *vcs* (D-F), grown at (A,D) 29°C; (B,E) 22°C; (C,F) 16°C. (G-L) Dark-field images of cleared first leaf showing the patterns of veins in L*er* (G,I,K) and *vcs* (H,J,L) grown for (G,H) 12 days at 22°C; (I,J) 11 days at 29°C; (K,L) 15 days at 16°C. (M,N) DIC images of the primary vein from leaves shown in G and H. (O,P) Cotyledon vein pattern of 12-day 22°C-grown L*er* (O) and *vcs* (P) show similar vein patterns, although cotyledon shape differs slightly. (Q,R) DIC images of the primary vein of cotyledons of L*er* (Q) and *vcs* (R), showing ectopic tracheary elements surrounding the *vcs* primary vein. Scale bars: (A-F) 50 μm; (G-L,O,P) 1 mm; (M,N,Q,R) 100 μm.

In contrast to leaves, the pattern of cotyledon veins was normal in *vcs* mutants (Fig. 3O-R). These observations indicated that VCS is required for normal patterning of internal tissues of the leaf, although growth at 16°C suppressed most defects.

We used SEM to further characterize 29°C-grown *vcs* mutant leaves (Fig. 4A-D). The *vcs* abaxial leaf surface was generally smooth, and surrounded by a small fringe of blade-like tissue (Fig. 4D). The *vcs* adaxial leaf surface was variable. Occasionally it appeared smooth (e.g. Fig. 4C), however more often it was highly convoluted and contained groups of raised cells with a terminal trichome (Fig. 4B,F,G). Normally, a trichome is surrounded at its base by a ring of trichome subsidiary cells (Fig. 4E). These groups of raised cells in the *vcs* leaves appeared similar to trichome subsidiary cells, although stacked in several layers and apparently arranged in cell files (Fig. 4F,G). These observations indicate that VCS is required for normal development of many different structures.

The wild-type leaf adaxial epidermis has a typical distribution of stomatal complexes and pavement cells, regardless of growth temperature (Fig. 4H-J). *vcs* mutants grown at 16 or 22°C showed similar adaxial leaf cell morphology (Fig. 4K,L), but those grown at 29°C did not have any recognizable pavement cells (Fig. 4M). The wild-type leaf abaxial epidermis is composed of stomata and smaller jigsaw-puzzle-shaped cells (Fig. 4N,P). *vcs* mutants grown at 16°C and 22°C appeared similar (Fig. 4Q,R), but those grown at 29°C were composed of small mostly rectangular cells, and occasional stomata (Fig. 4S). These observations indicated that both intermediate and low temperature growth suppressed *vcs* leaf epidermal defects.

VCS is required throughout leaf development

To determine when VCS was needed for normal leaf development, we carried out temperature shift experiments. We reasoned that if VCS was only required early, then shifting plants from low temperature to high temperature after leaf initiation may allow production of the suppressed leaf phenotype. Alternatively, if VCS was only required late, then shifting plants from high to low temperature after leaf initiation may allow production of the suppressed leaf phenotype. We germinated seedlings at 16°C (or 29°C), shifted a subset to 29°C (or 16°C) daily, and examined all the plants at day 14 (Fig. 5A). *vcs* mutants were smaller and more chlorotic the longer they were held at 29°C, regardless of whether the 29°C period was applied early or late in development. These data indicate that the 16°C treatment was required continuously for the suppressed phenotype.

We analyzed the effect of temperature shifts on leaf vein patterning (Fig. 5B, Fig. 6A). As observed in the intact plants, increased duration at 29°C resulted in a progressively decreasing vein pattern. However, instead of the broadly graded effects of the temperature shifts on overall leaf morphology, vein patterning had a critical need for the 16°C suppression early in leaf development. For plants shifted from 29°C to 16°C, areole formation decreased linearly in plants shifted between days 3 and 5, and was abolished in plants shifted on day 6 or later. For plants shifted from 16 to 29°C, significant areole formation only occurred in plants maintained at 16°C for at least their first 5 days.

To relate the early requirement for 16°C suppression to stages of leaf vascular development, we assessed leaf vascular tissue in cleared leaves of wild-type and vcs seedlings grown at either 29°C or 16°C for 2 to 7 days (Fig. 6B). In the wild type, primary vein procambium was detectable on day 3 (29°C) or day 4 (16°C), and differentiated primary veins were detectable on day 4 (29°C) or day 5 (16°C). Secondary vein procambium was detectable on day 4 (29°C) or days 6 (16°C). Differentiated secondary veins were detectable on day 5 (29°C)

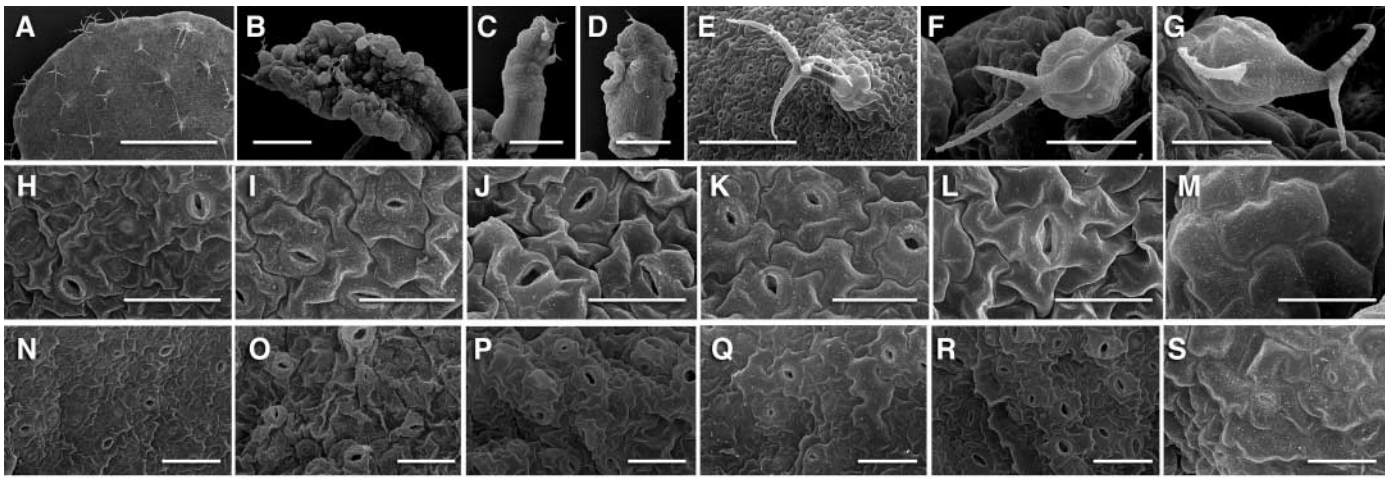

Fig. 4. SEM analysis of *vcs* leaf defects. (A) L*er* 9-day 29°C-grown; (B-D) *vcs* 9-day 29°C-grown, showing adaxial (B), side (C) and abaxial (D) views. (E-G) Trichome from 9-day 29°C-grown L*er* (E) and *vcs* (F-G) leaves. (H-M) Leaf adaxial cells; the images were taken at a position half way down the leaf and midway between the margin and the center of the leaf. Typical arrangements of stomatal guard cells and pavement cells are present in L*er* grown at 16°C for 15 days (H), 22°C for 12 days (I) and 29°C for 9 days (J), and in *vcs* grown at 16°C for 15 days (K) and 22°C for 12 days (L), however in *vcs* grown for 9 days at 29°C (M) no typical pavement cells could be detected. The abaxial leaf surface is typically uneven, and composed of stomatal guard cells and small irregularly shaped cells, such as shown for L*er* grown at 16°C for 15 days (N), 22°C for 12 days (O) and 29°C for 9 days (P). The abaxial leaf surface of *vcs* grown at 16°C for 15 days (Q) and 22°C for 12 days (R) appeared similar to the wild type. The abaxial surface of the 9-day 29°C-grown leaf (S) contained stomatal complexes, but no small irregularly shaped cells were present. Scale bars: (A) 1 mm; (B,C,D) 500 μm; (E) 200 μm, (F, G) 100 μm; (H-M) 40 μm, (N-S) 50 μm.

and day 7 (16°C). *vcs* mutant leaf vascular development showed similar timing for the primary vein in the 29°C grown plants. *vcs* mutants grown at 16°C were not distinguishable from the wild type prior to day 5, following this timepoint vascular development was at the same stage as observed for the wild type (data not shown). Taken together, the critical period for leaf secondary vein formation identified by the temperature shift coincided with times when the leaf would normally be forming secondary vein procambium.

Relationship between *VCS* and auxin signaling

Because the plant hormone auxin has been proposed to play roles in both leaf development and vein patterning, we used several approaches to explore the relationship between VCS and auxin signaling. First, we characterized *axr1-3 vcs-1* double mutants. *AXR1* encodes a ubiquitin E3 ligase-like protein that is required for activation of the SCF ubiquitin-protein ligase, which targets specific cellular proteins for degradation (Leyser et al., 1993; del Poze and Estelle, 1999; Gray et al., 1999; Gray et al., 2001). *axr1* mutants show reduced auxin responses, altered leaf shape, reduced apical dominance, and smaller hypocotyl vascular bundles (Estelle and Somerville, 1987; Lincoln et al., 1990). We found that *axr1-3* cotyledons contained reduced numbers of secondary veins [1.45 complete areoles and 0.7 incomplete areoles per cotyledon (n=67) in *axr1-3* compared to 3.1 complete and 0.8 incomplete areoles for Col-0 (n=45)], and that these cotyledon veins were often aberrantly positioned (Fig. 7C). The *axr1-3* leaf secondary veins were also reduced in number, frequently failed to intersect along the leaf margin, and isolated vascular islands were occasionally present (Fig. 7D). Growth temperature did not affect this vein pattern phenotype (data not shown).

We generated double mutants using the *axr1-3* allele, which is in the Col-0 ecotype. F2 from all crosses with Col-0 included some plants with a less-suppressed phenotype at low and intermediate temperatures. However, the *axr1-3 vcs-1* double mutants showed strong enhancement of cotyledon and leaf vein pattern defects. When grown at 16°C, *axr1-3 vcs-1* cotyledon secondary veins were free

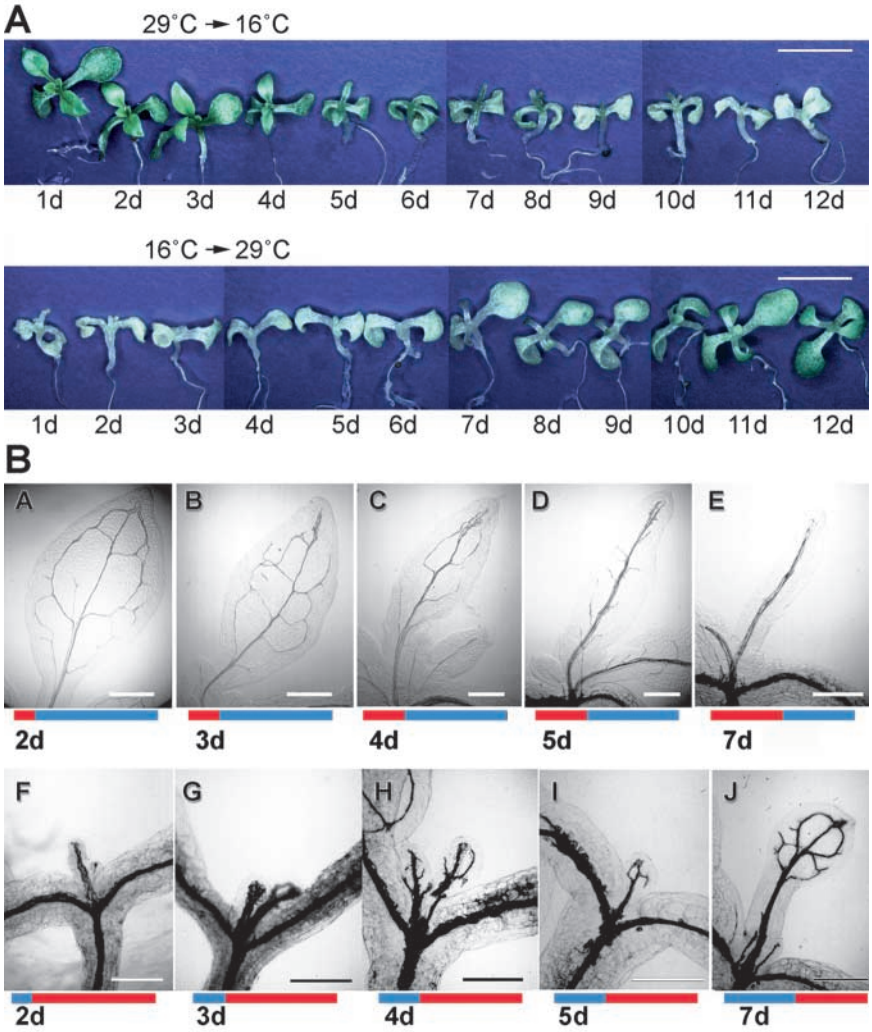

Fig. 5. Temperature shift experiments reveal a requirement for VCS throughout leaf development. (A) Seedling morphology of 14-day temperature-shifted *vcs* mutants. The top row shows plants germinated at 29°C and transferred to 16°C on the day indicated under each plant. The lower row shows plants germinated at 16°C, and transferred to 29°C. (B) Representative vein patterns from selected temperature shift time points. The red bars indicate the duration of time at 29°C, and whether this exposure was at the beginning or the end of the 14-day growth period. Scale bars: (A) 5 mm; (B) 200 μm.

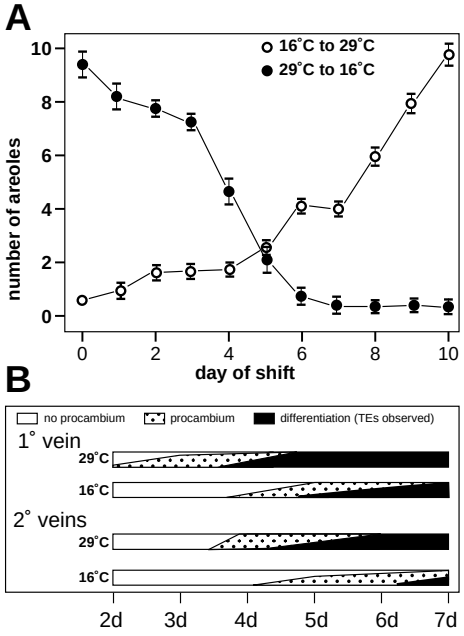

Fig. 6. Vascular development in leaves of temperature shifted and control plants.
(A) Counts of completed leaf areoles (a region fully delimited by veins) in the first leaves of 14-day temperature-shifted plants. Bars indicate the standard error of the mean, 18-26 leaves were examined for each time-point.
(B) Depiction of the developmental progression of primary and secondary veins in leaves of L*er* plants from a developmental time course carried out at 16°C or 29°C. For each time-point, the height of the white, stippled or black area represent the fraction of leaves with 1° or 2° veins totally absent (white), present only as procambium (stippled), or at least some of that vein class differentiated (black).

Table 2. Concentration of IAA that produced 50% relative inhibition of root elongation (I_{50}) for wild type and *vcs* mutants

	Wild type	*vcs*
16°C	3.2×10^{-8}	3.3×10^{-8}
29°C	2.9×10^{-8}	2.9×10^{-8}

I_{50} values shown are the mean values from two independent experiments (16°C), or three independent experiments (29°C).

ending (Fig. 7G), and the *axr1-3 vcs-1* double mutant leaves were small, containing only 1-3 veins (Fig. 7H). Growth at high temperatures resulted in further reduction of leaf size and vein pattern (data not shown). Enhancement of the *vcs* leaf defects by the loss of AXR1 indicated that signaling through the AXR1 pathway was at least partially intact in the *vcs* single mutant.

To examine intracellular patterns of biologically active auxin, we characterized DR5 expression in *vcs* mutants. DR5 contains synthetic auxin response elements fused to the GUS reporter gene (Ulmasov et al., 1997). Patterns of DR5 expression in developing *Arabidopsis* leaves have been well characterized (Aloni et al., 2003; Mattsson et al., 2003). At early leaf developmental stages, DR5 expression occurs in a spot at the distal end of the organ (Fig. 8A). As leaf development progresses, DR5 expression occurs within procambium and differentiating vascular tissues (Fig. 8B-C) (Aloni et al., 2003; Mattsson et al., 2003). In *vcs* mutants, DR5 expression was in similar positions as in wild type, with the caveat that fewer procambial strands and veins were present (Fig. 8D-F). At all stages of leaf development, GUS staining intensity appeared modestly reduced, especially at the hydathodes. Nevertheless, the similar patterns of DR5 expression in *vcs* and wild type suggests that pathways for auxin expression and movement within leaves is essentially intact.

To determine whether vcs mutants had intact auxin responses, we compared auxin inhibition of root elongation for wild type and *vcs* mutants (Estelle and Somerville, 1987). As shown in Table 2, *vcs* and wild type showed essentially identical I_{50} values, indicating that root perception and root response to auxin were not affected in *vcs* mutants. We also compared auxin inducibility of DR5 expression in the wild type and *vcs* mutants. DR5 expression was strongly induced in both the wild type and vcs mutants, regardless of growth temperature (Fig. 8G-J and data not shown); these results indicated that leaf auxin responses were intact in *vcs* mutants.

Finally, we examined the repercussion of perturbing auxin dynamics on *vcs* leaf development using the polar auxin transport inhibitor NPA (Fig. 9). In wild-type plants, growth in the presence of NPA resulted in occasional fused or lobed leaves, and all leaves had a pronounced midrib and a curled leaf blade with a wavy margin (Fig. 9B,J,R). These leaves contained a broad zone of disorganized vascular tissue subjacent to the leaf margin, and an increased number of secondary veins that coalesced to form a broad and poorly organized vein in the midrib region (Fig. 9F-V) (Sieburth, 1999; Mattson et al., 1999). When grown in the presence of NPA, *vcs* mutants also occasionally produced fused leaves (Fig. 9L). However, NPA-grown *vcs* mutants lacked the distinct

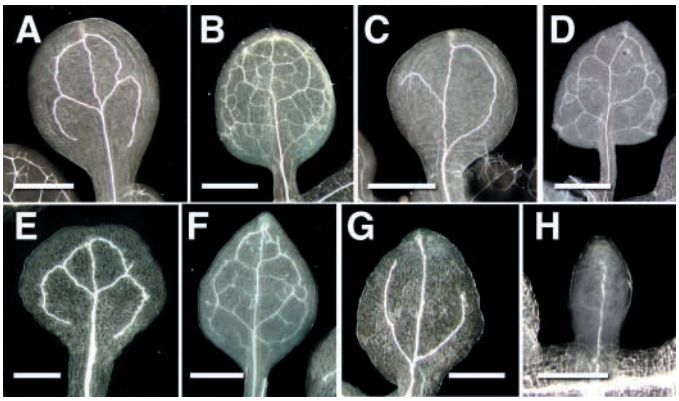

Fig. 7. Cotyledon and leaf vein patterns in *axr1-3*, *vcs*, and *vcs axr1-3* double mutants. All tissue is from 15-day 16°C-grown plants. Cotyledon (A,C,E,G) and leaf (B,D,F,H) vein patterns from L*er* (A,B), *axr1-3* (C,D), *vcs-1* (E,F), and *axr1-3 vcs-1* double mutants (G,H). Scale bars: 1 mm.

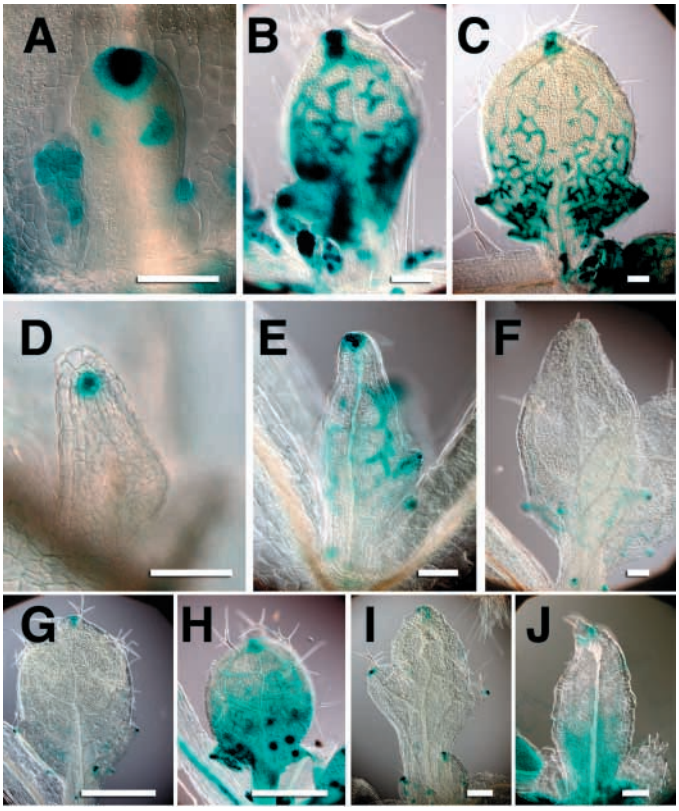

Fig. 8. DR5 expression and auxin inducibility in *vcs* leaves. DR5 expression in developing leaves of wild type (A-C) grown at 22°C (wild-type DR5 expression was similar regardless of growth temperature). (D-F) *vcs* mutants show DR5 expression at the distal end of the developing leaf (D, 29°C-grown) and in procambium (E,F, 22°C-grown). DR5 auxin induction was compared for 8-hour incubation in water (G,I) or 5 μM 2,4-D (H,J) in the wild type (G,H) and *vcs* (I-J). Data shown is for 29°C-grown tissue; similar results were observed for plants grown at 22°C and 16°C. Scale bars: (A-F) 100 μm; (G-J) 1 mm.

curled dark green blade seen in NPA-treated wild-type leaves, and instead their leaves were narrow with smooth margins

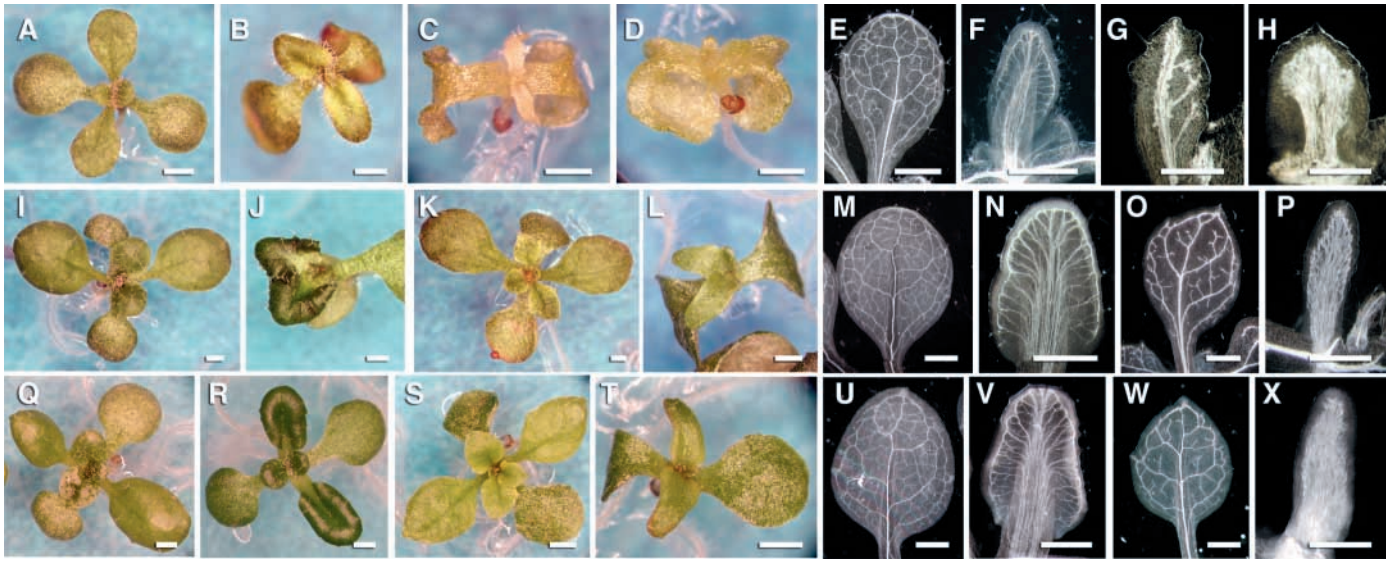

Fig. 9. *vcs* mutants show heightened sensitivity to polar auxin transport inhibitor NPA regardless of growth temperature. (A-H) 29°C-grown 9-day plants, (I-P) 22°C-grown 12-day plants, and (Q-X) 16°C-grown 15-day plants. (A,I,Q) L*er* controls and (B,J,R) L*er* grown in medium containing 1 μM NPA. (C,K,S) *vcs* controls and (D,L,T) *vcs* grown in 1 μm NPA. Dark-field images of cleared first leaves of L*er* and *vcs* grown for 9 days at 29°C (E-H), 12 days at 22°C (M-P) and 15 days at 16°C (U-X). L*er* controls (E,M,U), L*er* 1 μM NPA (F,N,V), *vcs* controls (G,O,W) and 1 μM NPA (H,P,X). Scale bars: 1 mm.

(Fig. 9D,L,T). The NPA-treated *vcs* leaves contained loosely organized veins that extended the length of the leaf, regardless of growth temperature (Fig. 9H,P,X). Both the morphology and the vein pattern of the NPA-grown *vcs* leaves bore a striking resemblance to the midrib regions of NPA-grown wild-type plants. These results suggested that normal development of the leaf lamina required both VCS and an activity disrupted by polar auxin transport inhibitors.

VCS encodes a putative WD-domain protein

To determine the molecular basis for the *vcs* mutant, we identified the *VCS* gene using map-based cloning (Fig. 10A). PCR-based codominant markers were used to position *VCS* to a 66 kb interval on chromosome 3 that contained 10 genes (Konieczny and Ausubel, 1993; Bell and Ecker, 1994; Jander et al., 2002). We sequenced candidate genes, and identified mutations in one gene, At3g13300 for all *vcs* alleles (Fig. 10B). Four were nonsense mutations, and one altered the conserved 3′ splice site (AG) of intron one. The phenotypic similarity of *vcs* alleles and the nature of these lesions suggested that these may be null alleles.

The *VCS* gene has 12 exons, and the Col-0 allele is predicted to encode a 1326 amino acid protein (Fig. 10B, Fig. 11). The VCS N terminus contains a proline-rich region (17/60 amino acids are proline), two well-conserved WD repeats, and a possible third less-conserved WD repeat (Fig. 11). We identified no intracellular targeting domains (e.g. NLS, transit sequence, signal sequence), suggesting that VCS might be cytoplasmically localized. The *Drosophila* and human genomes contain genes with 58 and 59% amino acid similarity over more than 94% of the *VCS* coding region, suggesting that VCS function may have been conserved during evolution. Functions of these homologs are not known. In addition, the adjacent gene (which we call *VARICOSE-RELATED*, *VCR*), At3g13290, is closely related; it shares 87% amino acid identity with *VCS* (Fig. 11).

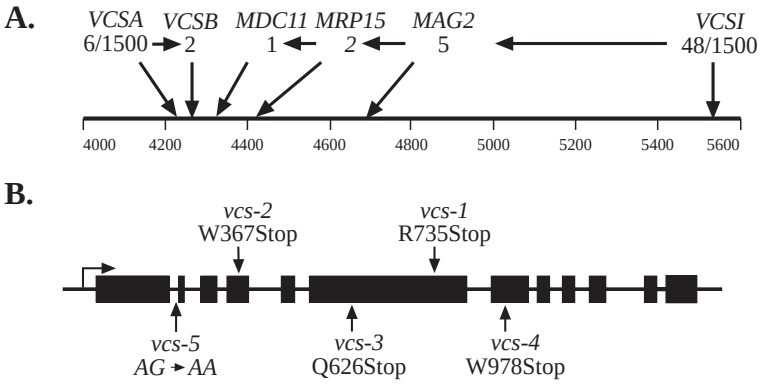

Fig. 10. Molecular identification of *VARICOSE*. (A) Mapping strategy within a 1.6 MB region of chromosome 3. The approximate positions of the polymorphisms used in this study for high resolution mapping of recombination breakpoints are indicated at the top. Using 750 *vcs* F2 mapping cross plants, we identified six recombinants at the polymorphism indicated as *VCSA*, and 48 at the *VCSI* polymorphism. The DNA from the plants containing recombinant chromosomes were further analyzed at polymorphisms *VCSB*, *MDC11*, *MRP15*, and *MAG2*. The number of chromosomes that were still heterozygous at each position is indicated. (B) Depiction of the *VCS* gene; black boxes represent exons, the arrow on the bar indicates transcription direction for orientation of the 5′ end of this gene. The position and nature of mutations in each *vcs* allele is indicated.

VCS expression

To determine which organs expressed *VCS*, we carried out RT-PCR experiments using RNA isolated from a variety of plant organs (Fig. 12A). We detected *VCS* RNA in all tissues examined, suggesting that *VCS* expression is wide-spread. We further characterized *VCS* expression using a GUS reporter gene fused to the sequences upstream of the *VCS* gene. Of the twelve lines characterized, two produced no GUS staining, and the remaining 10 produced the same staining pattern, albeit with differing intensity. In young seedlings, expression was present in the hypocotyl, leaf primordia and the cotyledon (Fig. 12B-D). Cotyledons showed strong expression in vascular tissues and in spots that corresponded to stomata. As leaves developed, the uniform staining pattern resolved into a vascular and spotted pattern similar to that of the cotyledons (Fig. 12E). The spots of high intensity expression in the leaves corresponded to trichomes, a subset of the stomata and vascular tissues (Fig. 12F-H). The vascular expression appeared to be in the phloem.

vcr mutants show normal seedling development

The sequence similarity of *VCS* and *VCR* suggested that they may carry out similar functions. Both *VCS* and *VCR* are expressed genes, as ESTs corresponding to each gene were identified in GenBank. To assess whether *VCR* plays essential roles in leaf development, we obtained an insertion allele from the Salk Institute's mapped T-DNAs (Salk_002338). This line contains a T-DNA insertion in intron 6. We verified the T-DNA insertion position by sequencing. We used PCR to identify *vcr/+* heterozygous plants, and examined siliques containing their self-pollinated progeny. Dissected siliques showed full seed set (data not shown), indicating that the loss of *VCR* did not affect female gametophyte or embryo development. Homozygous mutants, identified by PCR, also showed no defects throughout development.

```
                 *    *   **        *   * ***    ***  *           **
VCS      MASSPGNTNPHNTPPFDLGILFKPSSNPYPPPAASYPPPTGPFLHNQYDQQHYAPPGISA 60
VCR      MASSPGNTNPHNPPPFDLGTIFKPSSNPYPPP-------TGPFLNNQYNQQLYAPPGIAA 53
           *
VCS      QPSPVTQQQQDVSSSSAATNLHPQRTLSYPTPPLNLQSPRSNHNPGTHILALLNNTNNGA 120
VCR      QPSPVNQTQQDVSSSSSATNLQPQRTLSYPTPPLNPQSPRVNHNPGTHILALLN---NGG 110

VCS      PVANQEPSHQLPVVNHNEIARSFPGGSGPIRVPSCKLPKGRRLIGEHAVYDVDVRLQGEI 180
VCR      AVANQEPSH------HNEIARAFPGGSGPIHVPSGKMPKGRRLVGEHAVYDVDVRLQGEI 164

VCS      QPQLEVTPITKYGSDPQLVVGRQIAVNKVYICYGLKGGNIRVLNINTALRSLFRGHSQRV 240
VCR      QPQLEVTPITKYGSDPQLVLGRQIAVNKVYICYGLKGGSIRVLNINTALRSLFRGHSQRV 224

VCS      TDMAFFAEDVDMLASVSLDGKVFVWKISEGSEGEDQPQITGKIVLALQILGEEDTKHPRV 300
VCR      TDMAFFAEDVHLLASVSLDGKVFVWKISEGSEGDEQSQITGKIVVALQILGEEDTKHPRV 284

VCS      CWHCHKQEILVVSIGKHVLRIDTTKVGRGEVFSAEAPLQCPLDKLIDGVQIVGKHDGEVT 360
VCR      CWHCHKQEILVVSIGKHVLRIDTTKVGRGEVFSAEAPLQCHLDKLIDGVQIVGKHDGEVT 344

VCS      DLSMCQWMTTRLVSSSVDGTIKIWQDRKAQPLVVLRPHDGHPVSSATFVTSPERPDHIIL 420
VCR      DLSMCQWMTTRLVSSSVDGTVKIWQDRKTQPLVVLRPHDGLPVNSAIFVTSPERPDHIIL 404

VCS      ITGGPLNREMKIWVSAGEEGWLLPADAESWRCTQTLDLKSSTEPRAEEAFFNQVIALSEA 480
VCR      ITGGPLNREIKIWVSAGEEGWLLPADTESWRCTQTLDLKSSTEPQAEKAFFNQVIALSEA 464

VCS      GLLLLANAKRNALYAVHLDYGSSPVGTRMDYLSEFTVTMPILSFIGTNDPPEEPIVKVYC 540
VCR      GLLLLANARRNAIYSVHLDYGSSPVETLMDYLSEFTVTMPILSFIGTNDHPEEPFVKVYC 524

VCS      VQTLAIQQYTLDLCLCLPPPIENMGLEKSDSSVSREANLVEGMSEPSGLKPTDLPSVDSV 600
VCR      VQTLAIQQYTLDLFLCMPPPRENVGFEKSDSTVSREANLVESTLETSGMKPTELPSVGSV 584

VCS      PKPSIIVNRSESANKLSFPSAEATS----QAIVPPNGEPKTSGLPSQTSGAGSAYATLPQ 656
VCR      PKPSILVNRSENANMLSFPAGPASAGITPPAIVPPNGEPKTSGMPSETSDVDSAYAPSPQ 644

VCS      LPLSPRLSSKLSGYHTPVEAIEPVIPHHELGGKTPSADYSVDRQMDAVGERNLDVSSVEE 716
VCR      LPLSPRLSSKLSGYHTPVEAFEQVLPHHKLGGKTSSADYFYVRQTDDVGGRNLDVSSVEE 704

VCS      ISRSKDSNVTPDDDVSGMRSPSAFFKHPTHLVTPSEILMGVSSAEASITTEDRRDRDANI 776
VCR      NCRSKDTNVTPDDDVSGIRSPSAFFKQPTHLVTPSEILMGVSSTEASITTEDKRDRDANI 764

VCS      QDVNNDPRDTEVEVKEISEARSTQNGEINDHDETENCTSENREKVFCSQVSNLSTEMARD 836
VCR      EEVNNDARGLEVELKEVGEAQTSQNGEINYHETTENHTSESRENIFCSQASNLSTEMARD 824

VCS      CYPSTEGTFIPGESKAYGQPIKAGDESGVDSRGGPAKLLK-------------GKKQKAK 883
VCR      RHPITEGSAIPGDSMAYGQPLQAGDERGLDSRDVSAKLPESGSSSGLVATNSKGKKQKAK 884

VCS      NSQGPGLSSTSSNVANLADSFNEQSQSLSHPMTDLLPQLLAMQETMNQVMASQKEMQRQL 943
VCR      NSQGPGLSSTSSNVANLADSFNEQSQSLNHPMADLLPQLLALQETMTQVMASQKEMQRQL 944

VCS      SNAATGPIGKESKRLEVALGRMIEKSSKSNADALWARIQEETVKNEKALRDHAQQIVNAT 1003
VCR      SNAVTGPIVKEGKKLEVALGRMIEKSSKSNADALWAHFQEEAVKNEKALRDHGQQIMNET 1004

VCS      TNFMSKELNAMFEKTIKKELAAIGPALARSVVPVIEKTVSSAITESFQRGIGDKAVNQLD 1063
VCR      TNFTSKELNAMFEKTMKKEFASVGPTLARVVTPVIEKTVSSAITESFQRGIGDKAVNQLE 1064

VCS      KSVNIKLEATVARQIQAQFQTSGKQALQEGLRSSVESSVIPSFEKACKAMFDQIDSAFQK 1123
VCR      KSVNSKLETTVARQIQAQFQTSGRQVLQEGLRSSMESSVIPSFERSCKTMFEQVDSTLQK 1124

VCS      GIAEHTNESITSASSVAQALSRELAETQRNLLALAAAGANSGGSNSLVTQLSGGPLGALL 1183
VCR      GIGKHTSETISSASSVTQALNRELAESQRNRLALTAAGSN-----PLVTQLSNGPLGALL 1179

VCS      EKVEAPMDPTTELSRLISERKYEESFTSALQRSDVSIVSWLCSQVDLRGLLAMNPLPLSQ 1243
VCR      EKVEAPMDPTTELSRLISERKYEESFTSALQRSDVSIVSWLCSQVDLRGLLAMNPLPLSQ 1239

VCS      GVLLSLLQQLACDISKDTSRKLAWMTDVVAAINPSDQMIAVHARPIFEQVYQILHHHRNA 1303
VCR      GVLLSLLQQLACDISTDTSRKLGWMTDVVTAINPSDQMIAVHARPIFEQVYQILHHHRNA 1299

VCS      PGSDVSAIRLIMHVINSMLMGCK 1326
VCR      PGSDVSAVRLIMHVINSLLMSCK 1322
```

Fig. 11. Alignment of the *Arabidopsis* VCS and VCR amino acid sequences. Grey shading indicate amino acid identity. The N-terminal proline-rich domain is indicated by an asterisk above each proline of the VCS sequence. The two robust WD domains are indicated by boxes with solid lines, and the third less well conserved WD domain is indicated by a box with a dashed line.

Discussion

Plants produce leaves by a multi-step process that includes repressing expression of meristem identity genes, acquiring polarity, and leaf margin outgrowth. In recent years, genes with proposed roles in the first two steps, repression of meristem identity genes in the leaf primordium and establishment of adaxial/abaxial polarity, have been identified (Byrne et al., 2002; Semiarti et al., 2001; Eshed et al., 2001; McConnell et al., 2001; Kerstetter et al., 2001), and studies of these genes have led to a model for leaf development where adjacent adaxial and abaxial domains lead to both leaf blade outgrowth and patterning of internal leaf tissues. However, mechanisms driving leaf blade outgrowth and tissue patterning remain unclear. In this study, we characterized a mutant, *vcs*, which shows leaf and shoot apical meristem defects.

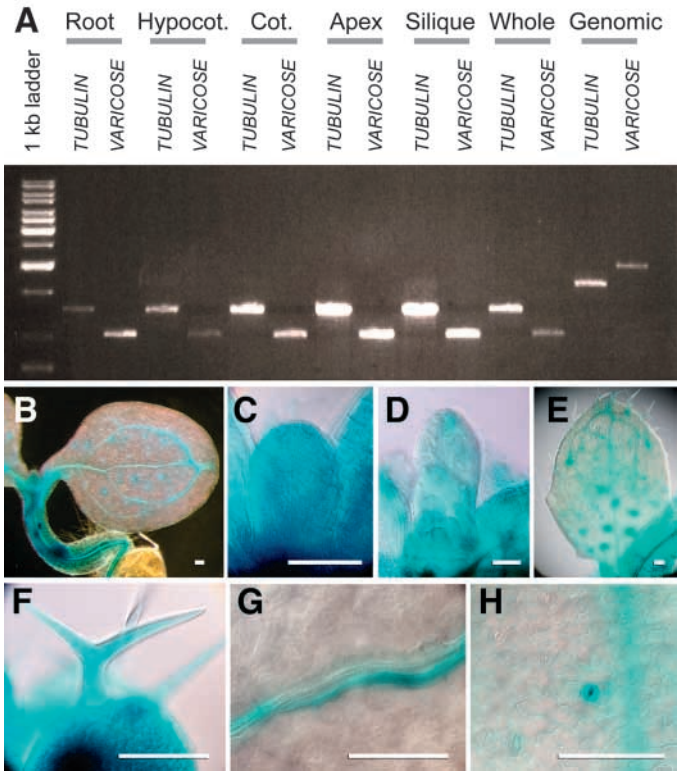

Fig. 12. *VCS* expression patterns. (A) RT-PCR analysis of *VCS* and α-tubulin (control) expression in RNA isolated from roots, hypocotyls, cotyledon, apices (leaves plus meristem), mixed age siliques, and entire seedlings (Whole). Genomic controls show the amplified fragment size that includes intron sequences. (B-H) GUS staining from a pVCS::GUS transgene. (B) 6-day cotyledon; (C) first leaf from a 4-day plant; (D) young leaves from a 9-day plant; (E) first leaf from a 9-day plant. (F) leaf trichome; (G) leaf vein; (H) stomata in the leaf. Scale bars: (B-H) 100 μm.

Does VCS encode a WD domain protein?

The *VCS* gene contained few sequence motifs that would suggest possible biochemical functions, with the exception of the two well-conserved WD repeats. WD repeats have been characterized structurally in the Gβ subunit of the trimeric G protein, where it assumes a seven-bladed propeller structure (Wall et al., 1995). Studies have highlighted the importance of the WD domain for protein-protein interactions, and the participation of these proteins in diverse processes (such as transcriptional repression and vesicle trafficking) (reviewed by Smith et al., 1999; Yu et al., 2000). However, theoretical calculations indicate that a minimum of four WD repeats are required to achieve a stable propeller configuration (Chothia et al., 1997), yet VCS contains only two robust WD repeats. Thus, if VCS does form a propeller-like structure, it must do so either by recruiting non-canonical WD repeats [such as has been suggested for TTG (Walker et al., 1999)] or through formation of a multimeric complex.

In *Arabidopsis*, a large number of WD domain- containing genes have been identified. For example, the *Pleiotropic regulatory locus 1*(*PRL1*) gene encodes a nuclear-localized WD domain protein and *prl1* mutants show pleiotropic phenotypes including defects in hormone signaling (Németh et al., 1998). Because WD domain proteins often have multiple different binding partners (e.g. van der Voorn and Ploegh, 1992; Holm et al., 2001) (reviewed by Smith et al., 1999), the pleiotropy of *vcs* (and *prl1*) mutants might be explained if their WD domains mediate interactions with multiple proteins and/or signaling pathways.

Temperature sensitivity of *vcs* alleles

Although the *vcs* phenotype was temperature dependent, four of the five *vcs* alleles were the result of premature stop codons, and one altered the 3′ splice site in the first intron. This result was surprising, as temperature sensitivity is most commonly associated with missense mutations that decrease the protein's thermostability, and the premature stop codons and splice site mutation we identified in the *vcs* mutants are likely to result in hypomorphic or null alleles. One explanation for *vcs* temperature sensitivity may be that there is a more stringent requirement for VCS function at high temperatures. For example, auxin levels are greater in plants grown at high temperature (Gray et al., 1998), and *vcs* temperature sensitivity might be explained if VCS functioned in a pathway that modified a response to elevated auxin levels. However, *vcs* mutants have apparently normal auxin responses. Nevertheless, it is possible that VCS functions in a different pathway that also has higher signal output at higher temperatures.

Alternatively, *vcs* temperature sensitivity could arise from a molecule or pathway that provides a functionally redundant activity. If a functionally redundant molecule is either less efficient, or requires a physical interaction that is thermally unstable, then the overall result could be phenotypic rescue under specific circumstances only, such as low temperature. VCR shares 87% amino acid identity with VCS, and thus is an attractive candidate to explain *vcs* temperature sensitivity. Although *vcr* mutants produced no discernable phenotype, a role for VCR in *vcs* temperature sensitivity cannot be ruled out until VCR function is assessed in the absence of VCS activity.

VCS and leaf development

Temperature shift experiments indicated a requirement for VCS throughout leaf development, however only a narrow developmental window allowed the development of leaf secondary veins. While previous descriptive studies have shown that secondary veins are normally established early during leaf development (Pyke et al., 1991; Tefler and Poethig, 1994), our data indicate that the secondary veins must be produced during this time period, as restoration of permissive conditions at later time points did not allow for secondary vein formation. These data might reflect a limited period of competence for leaf cells to produce, perceive and/or respond to vein formation signals.

By examining *vcs* leaf defects across a spectrum of growth temperatures, we found that internal leaf blade tissues (vascular and non-vascular) showed the greatest sensitivity to the loss of *VCS*. This observation suggests a direct role for VCS in normal patterning of internal leaf tissues. Internal tissue defects include both gross-level organizational defects (e.g. the disruption of palisade parenchyma and vein pattern), and control over cell proliferation (e.g. the increased number of xylem tracheary element cell files in veins of *vcs* leaves). That defects extended to several tissue types could either mean that VCS functions to coordinate the development of these leaf tissues or that multiple independent pathways within the leaf

require VCS. Future work to identify VCS binding partners should help to resolve this issue.

A severe loss of leaf blade was evident in *vcs* mutants grown in the presence of polar auxin transport inhibitors. In addition, this treatment reduced low-temperature suppression of the *vcs* phenotype. This reduced low-temperature suppression suggests that polar auxin transport inhibitors block an activity that provides functional redundancy with VCS. Although the simplest interpretation of these observations is that the partially redundant activity is polar auxin transport or a downstream pathway, we also note that auxin polar transport inhibitors disrupt general vesicle trafficking (Geldner et al., 2001). Thus, possible candidates for VCS redundancy remain numerous.

Current models of leaf formation propose that outgrowth of the leaf blade and lamina formation result from earlier events specifying leaf polarity. Although it is tempting to speculate that VCS may play a direct roles in leaf margin outgrowth, it is also possible that VCS function is more closely related to tissue formation, coordination of cell proliferation, or acquisition of cell identities within the lamina.

We thank Gary Drews, Mark Estelle, Bryan Pickett and Rebecca Frederick for useful discussions during the course of this work. We also gratefully acknowledge support from NSF (99-82876); NSERC (PDF to M.K.D.); NIH (DB training grant 5T32 HD07491 to J.P.); and the Arabidopsis Biological Resource Center for providing seed stocks. We thank the Salk Institute Genomic Analysis Laboratory for providing the sequence-indexed *Arabidopsis* TDNA insertion mutants; funding for the SIGnAL indexed insertion mutant collection was provided by the National Science Foundation.

References

Aloni, R. (1987). Differentiation of vascular tissues. *Annu. Rev. Plant Physiol.* **38**, 179-204.

Aloni, R., Schwalm, K., Langhans, M. and Ullrich, C. I. (2003). Gradual shifts in sites of free-auxin production during leaf-primordium development and their role in vascular differentiation and leaf morphogenesis in *Arabidopsis*. *Planta* **216**, 841-853.

Alonso, J. M., Stepanova, A. N., Leisse, T. J., Kim, C. J., Chen, H., Shinn, P., Stevenson, D. K., Zimmerman, J., Barajas, P., Cheuk, R. et al. (2003). Genome-wide insertional mutagenesis of Arabidopsis thaliana. *Science* **301**, 653-657.

Avsian-Ketchmer, O., Cheng, J.-C., Chen, L., Moctezuma, E. and Sung, Z. R. (2002). Indole acetic acid distribution coincides with vascular differentiation pattern during arabidopsis leaf ontogeny. *Plant Physiol*. **130**, 199-209.

Bell, C. J. and Ecker, J. (1994). Assignment of 30 microsatellite loci to the linkage map of *Arabidopsis*. *Genomics* **19**, 137-144.

Byrne, M. E., Barley, R., Curtis, M., Arroyo, J. M., Dunham, M., Hudson, A. and Martienssen, R. A. (2000). *Asymmetric leaves1* mediates leaf patterning and stem cell function in *Arabidopsis*. *Nature* **408**, 967-971.

Bryne, M. E., Simorowski, J. and Martienssen, R. A. (2002). *ASYMMETRIC LEAVES1* reveals *knox* gene redundancy in *Arabidopsis*. *Development* **129**, 1957-1965.

Carland, F. M. and McHale, N. A. (1996). *LOP1*: a gene involved in auxin transport and vascular patterning in *Arabidopsis*. *Development* **122**, 1811-1819.

Chen, Q., Atkinson, A., Otsuga, D., Christensen, T., Reynolds, L. and Drews, G. N. (1999). The *Arabidopsis FILAMENTOUS FLOWER* gene is required for flower formation. *Development* **126**, 2715-2726.

Chothia, C., Hubard, T., Brenner, S., Barns, H. and Murzin, A. (1997). Protein folds in the all-β and all-α classes. *Annu. Rev. Biophys. Biomol. Struct.* **26**, 597-626.

Chuck, G., Lincoln, C. and Hake, S. (1996). *KNAT1* induces lobed leaves with ectopic meristems when overexpressed in Arabidopsis. *Plant Cell* **8**, 1277-1289.

Clough, S. J. and Bent, A. (1998). Floral dip: A simplified method for *Agrobacterium*-mediated transformation of *Arabidopsis thaliana*. *Plant J*. **16**, 735-743.

del Pozo, J. C. and Estelle, M. (1999). The *Arabidopsis* cullin AtCUL1 is modified by the ubiquitin-related protein RUB1. *Proc. Natl. Acad. Sci. USA* **96**, 15342-15347.

Dellaporta, S. L., Wood, J. and Hicks, J. B. (1983). A plant DNA minipreparation: version II. *Plant Mol. Biol. Rep*. **1**, 19-21.

Deyholos, M. K., Cordner, G., Beebe, D. and Sieburth, L. E. (2000). The *SCARFACE* gene is required for cotyledon and leaf vein patterning. *Development* **127**, 3205-3213.

Donnelly, P. M., Bonetta, D., Tsukaya, H., Dengler, R. E. and Dengler, N. G. (1999). Cell cycling and cell enlargement in developing leaves of *Arabidopsis*. *Dev. Biol.* **215**, 407-419.

Eshed, Y., Baum, S. F., Perea, J. V. and Bowman, J. L. (2001). Establishment of polarity in lateral organs of plants. *Curr. Biol.* **11**, 1251-1260.

Estelle, M. and Somerville, C. (1987). Auxin-resistant mutants of *Arabidopsis thaliana* with an altered morphology. *Mol. Gen. Genet*. **206**, 200-206.

Geldner, N., Friml, J., Stierhof, Y.-D., Jürgens, G. and Palme, K. (2001). Auxin transport inhibitors block PIN1 cycling and vesicle trafficking. *Nature* **413**, 425-428.

Gray, W. M., Ostin, A., Sandberg, G., Romano, C. P. and Estelle, M. (1998). High temperature promotes auxin-mediated hypocotyl elongation in *Arabidopsis*. *Proc. Natl. Acad. Sci. USA* **95**, 7197-7202.

Gray, W. M., del Pozo, J. C., Walker, L., Hobbie, L., Risseeuw, E., Banks, T., Crosby, W. L., Yang, M., Ma, H. and Estelle, M. (1999). Identification of an SCF ubiquitin-ligase complex required for auxin response in *Arabidopsis thaliana*. *Genes Dev*. **13**, 1678-1691.

Gray, W. M., Kepinski, S., Rouse, D., Leyser, O. and Estelle, M. (2001). Auxin regulates SCF^{TIR1}-dependent degradation of AUX/IAA proteins. *Nature* **414**, 271-276.

Hay, A., Kaur, H., Phillips, A., Hedden, P., Hake, S. and Tsiantis, M. (2002). The gibberellin pathway mediates KNOTTED1-type homeobox function in plants with different body plans. *Curr. Biol*. **12**, 1557-1565.

Holm, M., Hardtke, C. S., Gaudet, R. and Deng, X.-W. (2001). Identification of a structural motif that confers specific interaction with the WD40 repeat domain of *Arabidopsis* COP1. *EMBO J.* **20**, 118-127.

Jander, G., Norris, S. R., Rounsley, S. D., Bush, D. F., Levin, I. M. and Last, R. L. (2002). Arabidopsis map-based cloning in the post-genome era. *Plant Physiol*. **129**, 440-450.

Kerstetter, R. A., Bollman, K., Taylor, R. A., Bomblies, K. and Poethig, R. S. (2001). *KANADI* regulates organ polarity in *Arabidopsis*. *Nature* **411**, 706-709.

Kim, G.-T., Shoda, K., Tsuge, T., Cho, K.-H., Uchimiya, H., Yokayama, R., Nishitani, K. and Tsukaya, H. (2002). The *ANGUSTIFOLIA* gene of *Arabidopsis*, a plant CtBP gene, regulates leaf-cell expansion, the arrangement of cortical microtubules in leaf cells and expression of a gene involved in cell-wall formation. *EMBO J*. **21**, 1267-1279.

Konieczny, A. and Ausubel, F. M. (1993). A procedure for mapping *Arabidopsis* mutations using co-dominant ecotype-specific PCR-based markers. *Plant J*. **4**, 403-410.

Leyser, H. M. O., Lincoln, C. A., Timpte, C., Lammer, D., Turner, J. and Estelle, M. (1993). Arabidopsis auxin-resistance gene AXR1 encodes a protein related to ubiquitin-activating enzyme E1. *Nature* **364**, 161-164.

Lincoln, C., Britton, J. H. and Estelle, M. (1990). Growth and development of the *axr1* mutants of *Arabidopsis*. *Plant Cell*. **2**, 1071-1081.

Maher, E. P. and Martindale, S. J. B. (1980). Mutants of Arabidopsis thaliana with altered responses to auxins and gravity. *Biochem. Genet*. **18**, 1041-1053.

Mattsson, J., Sung, Z. R. and Berleth, T. (1999). Responses of plant vascular systems to auxin transport inhibition. *Development* **126**, 2979-2991.

Mattsson, J., Ckurshumova, W. and Berleth, T. (2003). Auxin signaling in Arabidopsis leaf vascular development. *Plant Physiol*. **131**, 1327-1339.

McConnell, J. R. and Barton, M. K. (1998). Leaf polarity and meristem formation in *Arabidopsis*. *Development* **125**, 2935-2942.

McConnell, J. R., Emery, J., Eshed, Y., Bao, N., Bowman, J. and Barton, M. K. (2001). Role of *PHABULOSA* and *PHABOLUTA* in determining radial patterning in shoots. *Nature* **411**, 709-413.

Medford, J. I., Behringer, F. J., Callos, J. D. and Feldmann, K. A. (1992). Normal and abnormal development in the Arabidopsis vegetative shoot apex. *Plant Cell* **4**, 631-643.

Muday, G. K. and DeLong, A. (2001). Polar auxin transport: controlling where and how much. *Trends Plant Sci.* **6**, 535-542.

Németh, K., Salchert, K., Putnoky, P., Bhalerao, R., Koncz-Kálmán, Z., Stankovic-Stangeland, B., Bakó, L., Mathur, J., Okrész, L., Stabel, S., Geigenberger, P., Stitt, M., Rédei, G., Schell, J. and Koncz, C. (1998). Pleiotropic control of glucose and hormone responses by PRL1, a nuclear WD protein, in *Arabidopsis*. *Genes Dev.* **12**, 3059-3073.

Okada, K., Ueda, J., Komaki, M., Bell, C. and Shimura, Y. (1991). Requirement of the auxin polar transport system in early stages of Arabidopsis bud formation. *Plant Cell* **3**, 677-684.

Ori, N., Eshed, Y., Chuck, G. Bowman, J. L. and Hake, S. (2000). Mechanisms that control *knox* gene expression in the *Arabidopsis* shoot. *Development* **127**, 5523-5532.

Pyke, K. A., Marrion, J. L. and Leech, R. M. (1991). Temporal and spatial development of the cells of the expanding first leaf of *Arabidopsis thaliana* (L.) Heynh. *J. Exp. Bot.* **42**, 1407.

Reed, R. C., Brady, S. R. and Muday, G. K. (1998). Inhibition of auxin movement from the shoot into the root inhibits lateral root development in Arabidopsis. *Plant Physiol.* **118**, 1369-1378.

Ruegger, M., Dewey, E., Hobbie, L., Brown, D., Bernasconni, P., Turner, J., Muday, G. and Estelle, M. (1997). Reduced naphthylphthalamic acid binding in the tir3 mutant of Arabidopsis is associated with a reduction in polar auxin transport and diverse morphological defects. *Plant Cell* **9**, 745-757.

Running, M. P. (2002). Nuclear staining for confocal microscopy. In *Arabidopsis-A Laboratory Manual* (ed. D. Weigel and J. Glazebrook), pp. 100-103. Cold Spring Harbor, NY: Cold Spring Harbor Laboratory Press.

Sachs, T. (1981). The control of the patterned differentiation of vascular tissues. *Ad. Bot. Res.* **9**, 151-262.

Sakamoto, T., Kamiya, N., Ueguchi-Tanaka, M., Iwahori, S. and Matsuoka, M. (2001). KNOX homeodomain protein directly suppresses the expression of a gibberellin biosynthetic gene in the tobacco shoot apical meristem. *Genes Dev.* **15**, 581-590.

Semiarti, E., Ueno, Y., Tsukaya, H., Iwakawa, H., Machida, C. and Machida, Y. (2001). The *ASYMMETRIC LEAVES2* gene of *Arabidopsis thaliana* regulates formation of a symmetric lamina, establishment of venation and repression of meristem-related homeobox genes in leaves. *Development* **128**, 1771-1783.

Sieburth, L. E. (1999). Auxin is required for leaf vein pattern in Arabidopsis. *Plant Physiol.* **121**, 1179-1190.

Siegfried, K. R., Eshed, Y., Baum, S. F., Otsuga, D., Drews, G. N. and Bowman, J. L. (1999). Members of the *YABBY* gene family specify abaxial cell fate in *Arabidopsis*. *Development* **126**, 4117-4128.

Smith, T. F., Gaitatzes, C., Saxena, K. and Neer, E. J. (1999). The WD repeat: a common architecture for diverse functions. *Trends Biochem. Sci.* **24**, 181-185.

Telfer, A. and Poethig, R. S. (1994). Leaf Development. In *Arabidopsis* (ed. C. R. Somerville and E. Meyerowitz), pp. 379-403. Cold Spring Harbor, New York: Cold Spring Harbor Laboratory Press.

Timpte, C., Wilson, A. K. and Estelle, M. (1994). The *axr2-1* mutation of *Arabidopsis thaliana* is a gain-of-function mutation that disrupts and early step in auxin response. *Genetics* **138**, 1239-1249.

Tsuge, T., Tsukaya, H. and Uchimiya, H. (1996). Two independent and polarized processes of cell elongation regulate leaf blade expansion in *Arabidopsis thaliana* (L.) Heynh. *Development* **122**, 1589-1600.

Ulmasov, T., Hagen, G. and Guilfoyle, T. J. (1997). Aux/IAA proteins repress expression of reporter genes containing natural and highly active synthetic auxin response elements. *Plant Cell* **9**, 1963-1971.

van der Voorn, L. and Ploegh, H. L. (1992). The WD-40 repeat. *FEBS Lett.* **307**, 131-134.

Wall, M. A., Coleman, D. E., Lee, E., Iniguez-Lluhi, J. A., Posner, B. A., Gilman, A. G. and Sprang, S. R. (1995). The structure of the G protein heterotrimer Gi alpha 1 beta 1 gamma 2. *Cell* **38**, 1047-1058.

Walker, A. R., Davison, P. A., Bolognesi-Winfield, A. C., James, C. M., Srinivasan, N., Blundell, T. L., Esch, J. J., Marks, M. D. and Gray, J. C. (1999). The *TRANSPARENT TESTA GLABRA1* locus, which regulates trichome differentiation and anthocyanin biosynthesis in Arabidopsis, encodes a WD40 repeat protein. *Plant Cell* **11**, 1337-1349.

Yu, L., Gaitatzes, C., Neer, E. and Smith, T. F. (2000). Thirty-plus functional families from a single motif. *Protein Sci.* **9**, 2470-2476.